

# A high-power tapered and cascaded active multimode interferometer semiconductor laser diode\*

Lai Weijiang(赖伟江)<sup>1,†</sup>, Cheng Yuanbing(程远兵)<sup>1</sup>, Yao Chen(姚辰)<sup>1</sup>, Zhou Daibing(周代兵)<sup>2</sup>, Bian Jing(边静)<sup>2</sup>, Zhao Lingjuan(赵玲娟)<sup>2</sup>, and Wu Jian(伍剑)<sup>1</sup>

<sup>1</sup>Key Laboratory of Information Photonics and Optical Communication, Beijing University of Posts and Telecommunications, Beijing 100876, China

<sup>2</sup>Institute of Semiconductors, Chinese Academy of Sciences, Beijing 100083, China

**Abstract:** A high power semiconductor laser diode with a tapered and cascaded active multimode interferometer (MMI) cavity was designed and demonstrated. An output power as high as 32 mW was obtained for the novel laser diode with a tapered and cascaded active MMI cavity, being much higher than the 9.8 mW output power of the conventional single ridge F-P laser with the same material structure and the same device length due to the larger active area; and also being higher than the 21.2 mW output power of the rectangular and cascaded active MMI laser diode with nearly the same structure, except for the shape of the MMI area. In addition, the tapered and cascaded active multimode interferometer laser showed stable single mode outputs up to the maximum output power.

**Key words:** taper-shape MMI; 3D BPM; self-image principle; high-power LD

**DOI:** 10.1088/1674-4926/32/5/054007

**PACC:** 7820; 4260B; 4260D

## 1. Introduction

High power semiconductor edge-emitting laser diodes (LDs) have become important and attractive devices in a wide variety of applications, such as pumping sources of optical fiber amplifiers, wavelength conversion with second harmonic generation, medicine, printing and manufacturing. In order to increase the output power of semiconductor laser diodes, several approaches have been proposed<sup>[1]</sup>, such as adopting strained multi-quantum-well (MQW) as the gain material<sup>[2,3]</sup>, and utilizing broad area structures and tapered waveguide structures for LDs<sup>[4]</sup>. A combination of the above approaches is, therefore, a promising approach towards achieving a practical solution for high power operation.

A semiconductor laser with an active MMI cavity is one of the most promising broad area structures. Active MMI offers high power in addition to regular single-mode output, which can be coupled into a standard single mode fiber without using an additional output mode trimming device. The MMI, which is one of the passive devices based on the self-image principle<sup>[5]</sup>, has been widely used in optical communication as a power and wavelength combiner, splitter, etc. However, an MMI used as an active device was first developed by Hamamoto *et al.* in 1997<sup>[6]</sup>. It shows a significant reduction in driving voltage, as well as an increase in optical output power compared to regular single-stripe LDs. In 1998, a laser diode with a cascaded and rectangular MMI cavity was developed to increase the output power further<sup>[7-10]</sup>. Thereafter, active MMIs were widely used to increase the output power of SLDs, SOAs, etc.<sup>[11,12]</sup>.

Here, a high power semiconductor laser diode is designed

and fabricated using a combination of the above approaches, such as using strained InGaAs/InGaAsP MQW as the gain material, adopting a tapered and cascaded active MMI cavity for the first time. The three dimensional beam propagation method (3D-BPM) was used to lead a proper waveguide design for stable single-mode operation at the output of the active-MMI configuration. For comparison, regular single stripe LDs of 4  $\mu\text{m}$  width and LDs with cascaded and rectangular MMI cavity were also fabricated simultaneously on the same wafer. The cavity length was 750  $\mu\text{m}$  for all structures.

## 2. Design and fabrication

### 2.1. Principle of tapered MMI

A schematic concept of the tapered active MMI LD is shown in Fig. 1. This consists of conventional single-mode waveguides that are connected to a  $1 \times 1$  tapered MMI

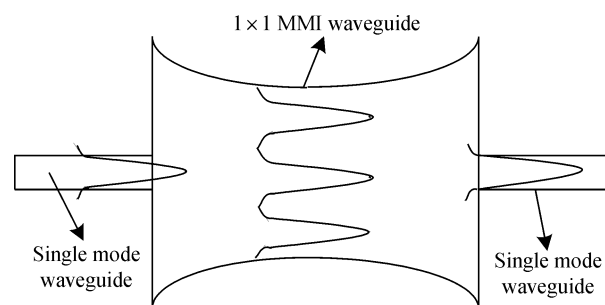


Fig. 1. Concept of tapered MMI.

\* Project supported by the State Key Development Program for Basic Research of China (Nos. 2006CB604901, 2006CB604902), the National High Technology Research and Development Program of China (Nos. 2009AA01Z256, 2008AA01331), and the National Natural Science Foundation of China (Nos. 61006041, 61001121, 60736036).

† Corresponding author. Email: laiweijiang@semi.ac.cn

Received 16 October 2010, revised manuscript received 14 December 2010

© 2011 Chinese Institute of Electronics

Table 1. Parameters used in the BPM simulation.

Layer	Wavelength ( $\mu\text{m}$ )	Thickness (nm)	Effective index
InP buffer	0.92	560	3.167
InGaAsP SCH layer	1.2	120	3.338
4 pairs MQW	Well (-0.1%)	6	3.482
	Barrier (0.2%)	10	3.338
InGaAsP SCH layer	1.2	120	3.338
InP clad layer	0.92	160	3.167
InGaAsP etch stop layer	1.2	20	3.338
InP clad layer	0.92	1800	3.167
InGaAs contact layer	1.65	200	3.482

coupler.

The principle of “self-imaging” allows for input images to be repeated along the device length. For the tapered MMI,  $L_{\text{MMI-T}}$ , the length to obtain the first appearance of  $N$  images is given as<sup>[13]</sup>

$$L_{\text{MMI-T}} = \frac{1}{c} L_{\text{MMI-R}}, \quad (1)$$

$$L_{\text{MMI-R}} = \frac{4nW_R^2}{Nl}, \quad (2)$$

where  $L_{\text{MMI-R}}$  is the length to obtain the first appearance of  $N$  images in a regular rectangle MMI. So the length of the tapered MMI can be reduced by  $\frac{1}{c}$  ( $c > 1$ ). In other words, if they have the same length of the MMI area, the tapered MMI exhibits a larger active area than the regular rectangle MMI, which could improve the quantum efficiency and increase the output power of the LD.

Meanwhile, the driving voltage of the laser diodes can be considered as follows<sup>[9]</sup>,

$$V \approx V_{\text{th}} + IR, \quad (3)$$

$$R \approx R_1 + R_2 \approx R_1 + \frac{rd}{\text{Area}} \propto \frac{1}{\text{Area}}, \quad (4)$$

where  $V_{\text{th}}$  is voltage at threshold,  $I$  is the current,  $R$  is the series resistance,  $R_1$  is the contact resistance, and  $R_2$  is the bulk resistance.

Therefore, a larger active area also contributes to a reduction in  $R$ , which results in a lower driving voltage.

## 2.2. Design

The material structure of the LD is shown in Table 1. Strained MQWs were used as the active layers of the LD in order to obtain a high material gain. The MQWs consist of 4 pairs of undoped 6 nm -0.1% compressive strain InGaAs wells separated by 10 nm 0.2% tensile strain InGaAsP (1.2*Q*) barriers, sandwiched between 120 nm lattice-matched InGaAsP (1.2*Q*) optical confinement layers.

The schematic structure of the tapered and cascaded active-MMI LD is shown in Fig. 2. Two cascaded 1 × 1 multimode interference couplers are connected to regular single-mode waveguides to obtain high power with regular single-transverse-mode output. The width of the MMI is tapered. As shown in Fig. 2, the length of the single-mode waveguide, tapered MMI area is  $L_1, L_2, L_3, L_t$ , while the width is  $W, W_1,$

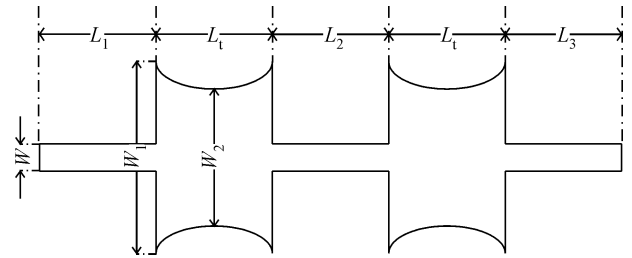


Fig. 2. Schematic of the ridge waveguide of the cascaded and tapered MMI.

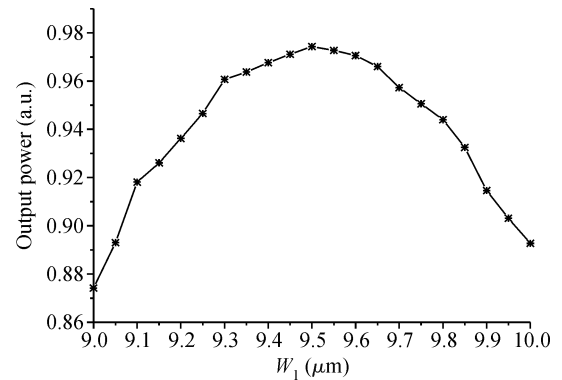


Fig. 3. Output power at the end of the single-mode waveguide with the change of  $W_1$ .

$W_2$ , respectively.  $W$  was set to 4  $\mu\text{m}$  in order to get a single transverse mode output,  $L_1, L_2, L_3, L_t$  are all equal to 150  $\mu\text{m}$ , and the total length of the device is 750  $\mu\text{m}$ .

The transmission of the optical field in the waveguide was simulated by 3D-BPM.  $W_1$  and  $W_2$  were considered as variable parameters.

In the simulation, we first used the fundamental mode of the single-mode waveguide as the input optical field. Then we set  $W_2 = 7.5 \mu\text{m}$ ,  $W_1 = 9.0-10.0 \mu\text{m}$ , and calculated the output power at the end of the single-mode waveguide with the change of the  $W_1$ . The result is shown in Fig. 3.

When  $W_1 = 9.5 \mu\text{m}$ , the output power has a maximum and the waveguide loss is about 0.11 dB.

Figure 4 shows the output field mode at the end of the single-mode waveguide when  $W_1 = 9.5 \mu\text{m}$ ,  $W_2 = 7.5 \mu\text{m}$ . It shows a single transverse mode output.

In comparison, we also fabricated a sing-strip F-P LD and a cascaded rectangle MMI LD, in which the width of the MMI

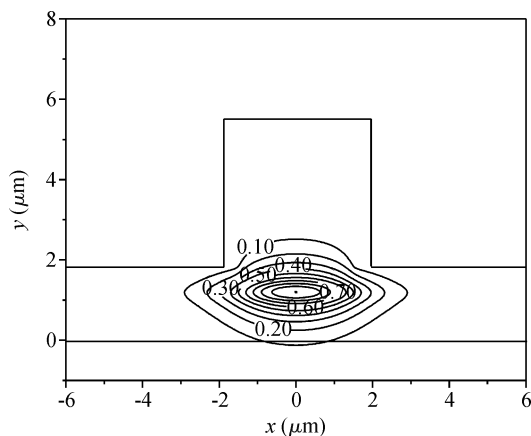


Fig. 4. Output optical field mode at the end of the single mode waveguide.

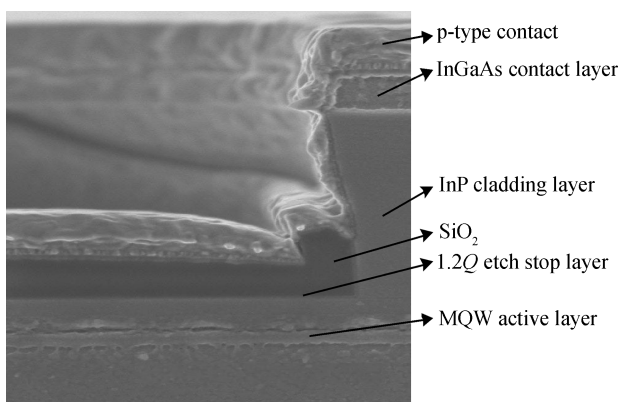


Fig. 5. Cross section of the ridge of the tapered MMI LD.

area was  $8 \mu\text{m}$ . The detail of the simulation is not listed. The total gain areas of the above devices were  $2.8 \times 10 \mu\text{m}^2$ ,  $4.2 \times 10 \mu\text{m}^2$  and  $4.8 \times 10 \mu\text{m}^2$ , respectively.

### 2.3. Fabrication

The fabrication process of the device is the same as that of the conventional F-P LD. The material of the LD is grown by MOCVD based on an n-type InP substrate. The 20 nm InGaAsP (1.2Q) in the middle of the InP cladding layer is used as an etch stop layer. The ridge is etched first by UV photolithography, and then by the Bbromine and HCl. Then  $4000 \text{ \AA}$  SiO<sub>2</sub> is grown on top of the InGaAs contact layer. Another photolithography process is used in order to open the SiO<sub>2</sub> windows on the top of the ridge. Then Au/Ti/Pt is deposited as the p-type electrode, and Ge/Ni/Au as the n-type electrode. The cross section of the ridge of the LD is shown in Fig. 5.

### 3. Results and discussion

Figure 6 is the microscope photos of the single-strip LD, cascaded rectangle MMI LD and cascaded tapered MMI LD.

We tested the output power of the devices with a thermal-control circuit. The output power against current and voltage against current characteristics are shown in Fig. 7. The tem-

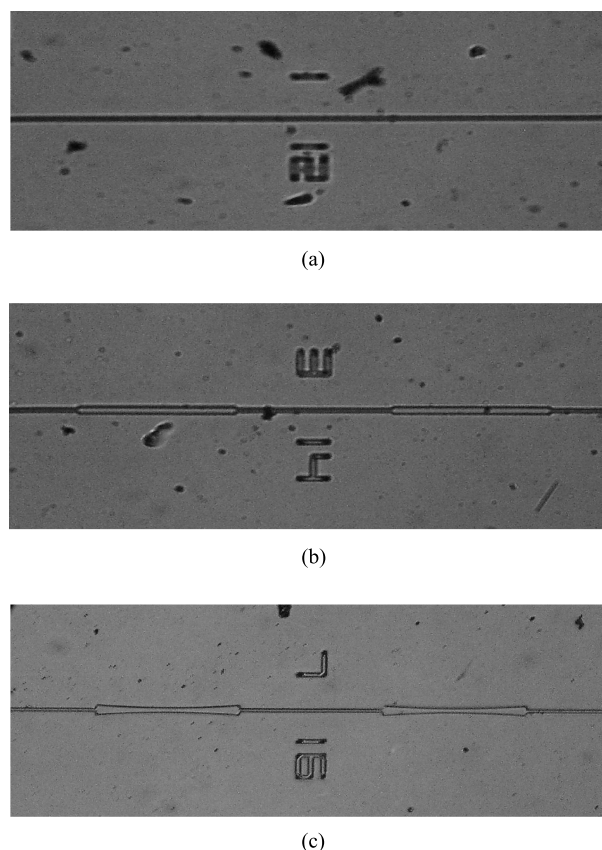


Fig. 6. (a) Single strip LD. (b) MMI LD with cascaded and rectangular cavity. (c) MMI LD with cascaded and tapered cavity.

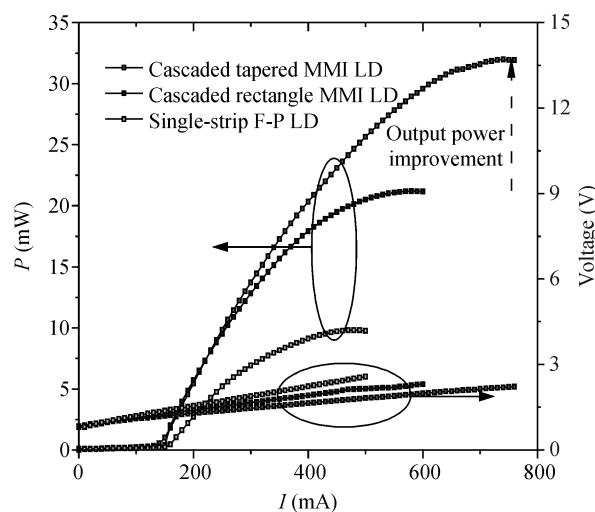


Fig. 7. Output power against current and voltage against current characteristics.

perature is fixed at  $25 \text{ }^\circ\text{C}$ . The output power of the single-strip LD is up to 9.8 mW, the saturation current is about 450 mA, and the resistance is about  $3.3 \Omega$ . The result of the rectangle MMI LD is 21.2 mW, 600 mA and  $2.2 \Omega$ , respectively. For the tapered MMI LD, the output power is up to 32 mW, the saturation current is about 780 mA, and the resistance is  $1.5 \Omega$ .

As we can see, because of the tapered MMI LD's larger active area, its output power shows a 10.8 mW improvement

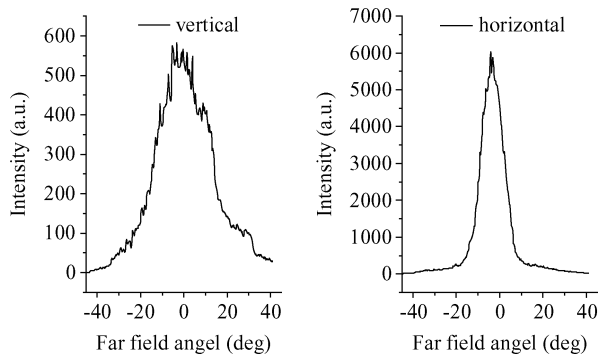


Fig. 8. Far field patterns of the rectangular MMI LD.

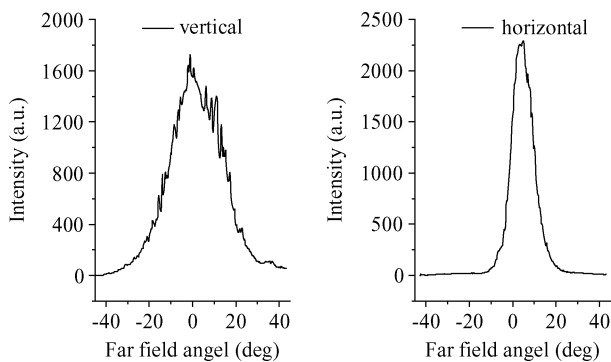


Fig. 9. Far field patterns of tapered MMI LD.

compared to the rectangular MMI LD.

The far field patterns of the rectangular MMI LD and the tapered MMI LD are shown in Figs. 8 and 9. The left picture is the vertical image and the right is the horizontal image. This shows a stable single-mode output.

#### 4. Conclusion

A cascade taper-shaped MMI LD is demonstrated for the first time. A high output power of 32 mW is achieved, corresponding to a 10.8 mW improvement compared to the regular rectangular MMI LD. The saturation current is up to 780 mA, and the resistance is only 1.5  $\Omega$ , which lead to a low power consumption. Under continuous-wave operation at regular room

temperature (25  $^{\circ}\text{C}$ ), it shows stable single-mode output characteristics.

#### References

- [1] Islam M N. Raman amplifiers for telecommunications vol. 1: physical principles. Chapter 5. New York: Springer, 2003
- [2] Thijs P J A, Tiemijer L F, Kuindersma P I, et al. High performance of 1.5  $\mu\text{m}$  wavelength InGaAs–InGaAsP strained quantum-well lasers and amplifiers. *IEEE J Quantum Electron*, 1991, 27: 1426
- [3] Thijs P J A, Tiemijer L F, Binsma J J M, et al. Progress in long-wavelength strained-layer InGaAs(P) quantum-well semiconductor lasers and amplifiers. *IEEE J Quantum Electron*, 1994, 30: 477
- [4] Bisping D, Pucicki D, Fischer M, et al. GaInNAs based high-power and tapered laser diodes for pumping applications. *IEEE J Sel Topics Quantum Electron*, 2009, 9(5): 968
- [5] Soldano L B, Pennings E C M. Optical multi-mode interference devices based on self-imaging principles and applications. *J Lightwave Tech*, 1995, 13(4): 615
- [6] Hamamoto K, Gini E, Holtmann C, et al. Single transverse mode active MMI 1.5  $\mu\text{m}$  InGaAsP buried-hetero laser diode. 8th European Conf on Integrated Optics, Stockholm, Sweden, 1997: 1
- [7] Hamamoto K, Gini E, Holtmann C, et al. Single transverse mode active multimode interferometer InGaAsP/InP laser diode. *Electron Lett*, 1998, 34(5): 463
- [8] Hamamoto K, Gini E, Holtmann C, et al. Single transverse mode active multimode interferometer 1.45  $\mu\text{m}$  high power laser diode. *Appl Phys B*, 2001, (73): 571
- [9] Hamamoto K, Naniwae K, Ohya M. High power with low electric power consumption active multi-mode interferometer laser diode for fiber amplifier. *Electron Lett*, 2002, 38(43): 517
- [10] Hamamoto K, Ohya M, Naniwae K, et al. Low wall-plug consumption laser diodes by using active multimode interferometer (MMI). *IEEE 19th International Semiconductor Laser Conference*, 2004
- [11] Zang Z, Minato T, Navaretti P, et al. High-power (> 110 mW) superluminescent diodes by using active multi-mode interferometer. *IEEE Photonics Technol Lett*, 2010, 22(10): 721
- [12] Hamamoto K, Gini E, Holtmann C, et al. Active multi-mode interferometer semiconductor optical amplifier. *OSA/OAA (Optical Amplifiers and Their Applications)*, Québec, Canada, 2000
- [13] Levy D S, Scarmozzino R, Osgood Jr R M. Length reduction of tapered  $N \times N$  MMI devices. *IEEE Photonics Technol Lett*, 1998, 10(6): 830